Journal of Inorganic Biochemistry 260 (2024) 112685

Contents lists available at ScienceDirect

Journal of Inorganic Biochemistry

journal homepage: www.elsevier.com/locate/jinorgbio

Polyimidazole ligands: Copper(II) complexes and antiproliferative activity in cancer cells

Fabrizia Brisdelli [a], Noemi Bognanni [b], Alessandra Piccirilli [a], Mariagrazia Perilli [a], Denise Bellotti [c], Maurizio Remelli [c], Graziella Vecchio [b,*]

[a] Dipartimento di Scienze Cliniche Applicate e Biotecnologiche, Università degli Studi dell'Aquila, via Vetoio, Coppito 67100, L'Aquila, Italy
[b] Dipartimento di Scienze Chimiche, Università degli Studi di Catania, V.le A. Doria 6, 95125 Catania, Italy
[c] Dipartimento di Scienze Chimiche, Farmaceutiche ed Agrarie, Università degli Studi di Ferrara, via L. Borsari 46, 44121 Ferrara, Italy

ARTICLE INFO

Keywords:
Chelation therapy
Cytotoxicity
Imidazole
Pyridine
ROS
Tumor

ABSTRACT

The design of novel chelators for therapeutic applications has been the subject of extensive research to address various diseases. Many chelators can manipulate the levels of metal ions within cells and effectively modulate the metal excess. In some cases, chelators show significant toxicity to cells.

We investigated polyimidazole ligands by potentiometry and UV–Vis spectroscopy for their ability to form copper(II) complexes. We also compared the antiproliferative activity of the polyimidazole ligands and their copper(II) complexes with polypyridine ligands in CaCo-2 (colorectal adenocarcinoma), SH-SY5Y (neuroblastoma) and K562 (chronic myelogenous leukemia) cells and normal HaCaT (keratinocyte) cells.

Polyimidazole ligands are less cytotoxic than their analogous polypyridine ligands. All polyimidazole ligands, except the tetraimidazole ligand for K562 cells, did not show any significant effect on the viability of cancer and normal cells. In contrast, the cytotoxic activity of polypiridine ligands was also observed in normal cells with IC_{50} values similar to those of cancer cells.

Tetraimidazole ligand, the only ligand active on the leukemic K562 cell line, induced caspase-dependent apoptosis and increased intracellular reactive oxygen species production with mitochondrial damage.

The low cytotoxicity of the polyimidazole ligands, even if it limits their use as anticancer agents, could make them useful in other medical applications, such as in the treatment of metal overload, microbial infections, inflammation or neurodegenerative disorders.

1. Introduction

The design of novel chelators for therapeutic applications has been the subject of extensive research to address various diseases. Many chelators can manipulate the levels of metal ions within cells and effectively modulate the metal excess. This ability has spurred the development of a class of compounds known as Metal Protein-Attenuating Compounds, which hold promise as potential therapeutic agents for restoring metal homeostasis [1–3]. Generally, the aim is to design a non-toxic ligand with a high affinity for essential metals such as iron, zinc, and copper. Such ligands could serve as candidates for metal-based drugs or exploit their potential to mobilize these metals from intracellular storage sites.

Specifically, copper is an essential co-factor of several cuproenzymes

Abbreviation: Ac-DEVD-AMC, acetyl-Asp-Glu-Val-aspaminomethylcoumarin; Ac-IETD-AFC, acetyl-Ile-Glu-Thr-Asp-aminotrifluoromethylcoumarin; Ac-LEHD-AMC, acetyl-Leu-Glu-His-Asp-aminomethylcoumarin; BisIM N,N′, Bis(4-imidazolylmethyl)-ethylenediamine; Bispicen N,N′, Bis(2-pyridymethyl)-ethylenediamine; t-BHP, tert-butylhydroperoxide; CCCP, carbonyl cyanide *m*-chlorophenylhydrazone; $DCFH_2$-DA, 2′,7′-dichlorofuorescein diacetate; DMEM, Dulbecco's modified Eagle's medium; D-pen, D-penicillamine; DTT, dithiotreitol; EDTA, ethylenediamine tetraacetic acid; EGTA, Ethyleneglycol- bis(β-aminoethyl)-N,N,N′,N′-tetraacetic Acid; JC-1 5,5′,6,6′, Tetrachloro-1,1′,3,3′-tetraethylbenzimidazolylcarbocyanine, iodide; MMP, mitochondrial membrane potential; MTT 3, (4,5-dimethylthiazol-2-yl)-2,5-diphenyltetrazolium bromide; RPMI, Roswell Park Memorial Institute; ROS, reactive oxygen species; TetraIM N,N,N,N′, tetra((imidazol-4- yl)-methyl)-ethylenediamine; TPEN, N,N,N′,N′, tetrakis(2-pyridylmethyl)ethylenediamine; Trien, trientine; TrisIM N,N,N′, tris((imidazol-4-yl)methyl)-ethylenediamine; Trispicen N, N,N′, Tris(2-pyridylmethyl)-ethylenediamine); TM, tetrathiomolybdate.

* Corresponding author.
E-mail address: gr.vecchio@unict.it (G. Vecchio).

https://doi.org/10.1016/j.jinorgbio.2024.112685
Received 24 May 2024; Received in revised form 11 July 2024; Accepted 29 July 2024
Available online 30 July 2024

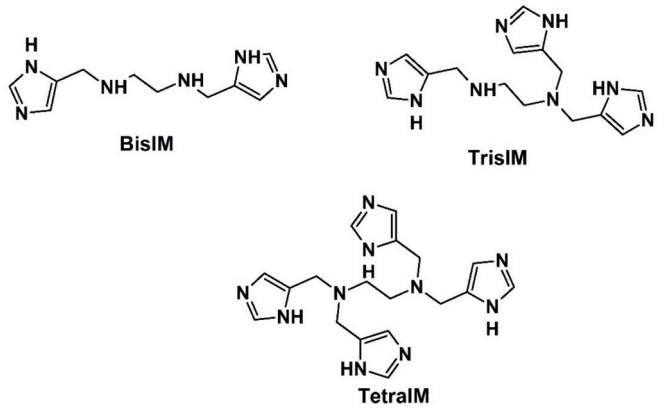

Fig. 1. Investigated polyimidazole ligands.

that have a critical role in the different biological processes in mammals, such as oxidative phosphorylation (cytochrome *c* oxidase), antioxidative activity (SOD1) and signaling. Moreover, Cu ions are involved in Fenton reactions, which can produce reactive oxygen species (ROS) [4].

Copper is pivotal in promoting angiogenesis, cancer growth, and metastasis. Recent research has delved into the involvement of copper-binding proteins in cancer progression [5–7]. Recognizing copper roles in cancer, disrupting copper trafficking has emerged as a viable therapeutic strategy [7–9], leading to the development of copper-specific ligands for anticancer therapies [8,10–12].

Some representative examples of well-known Cu chelators include D-penicillamine (D-pen), tetrathiomolybdate (TM) and trientine (trien) used in clinical to reduce copper levels in Wilson disease, which also show anticancer activity [9,13].

Clinical studies have investigated the use of TM as an anticancer agent. Notably, TM has shown promise in certain types of brain cancer where copper levels are elevated [14,15].

Moreover, TM has been explored in combination with cancer therapies [15,16]. It has been proven that reducing copper levels with TM can enhance the effectiveness of existing chemotherapy agents. This synergy may arise because copper plays a role in DNA repair and antioxidant defenses, and reducing copper levels could sensitize cancer cells to chemotherapy-induced DNA damage.

D-pen ($\log\beta_{CuL}$ = 18.8) has been studied in combination with cisplatin to improve its efficacy in platinum-resistant tumors [17]. Trien ($\log\beta_{CuL}$ = 20.1) can suppress neovascularization and increase apoptosis in cancer cells [13].

Polypyridine ligand TPEN (N,N,N′,N′-tetrakis(2-pyridylmethyl)ethylenediamine), known for its high affinity for copper ions, has also been examined for its toxic effects on cancer cells [18–22]. The antiproliferative and apoptotic activity of TPEN was previously described in several cell systems such as lymphocytes [23], malignant epithelial cells [24], leukemia [20], colon cancer [25], ovarian [26] and breast cancer [27]. The cytotoxic effect of the other polypyridine ligands, Trispicen (N,N,N′-tris(2-pyridylmethyl)-ethylenediamine) and Bispicen (*N*,*N*′-bis (2-pyridymethyl)-ethylenediamine) has so far been observed only in normal peripheral blood lymphocytes [28].

Despite the reported cytotoxicity, polypyridine ligands have found utility in various biological applications due to their exceptional complexation capabilities [29–31].

Recently, we synthesized the polyimidazole ligands analogous to the TPEN, Trispicen and Bispicen [32]. Imidazole is a common side chain found in proteins, often acting as a coordinating site for metal ions. Additionally, the imidazole moiety is a fundamental structural element in various medical scaffolds [33].

Polyimidazole ligands may be of interest for their use in biological systems. Such compound is *N*,*N*′-bis(4-imidazolylmethyl)-ethylenediamine (BisIM) and its metal complexes, which have been investigated, with reported high stability constants, particularly for 3d metal ions [34]. The copper(II) complex with BisIM exhibits high stability constant [34], closely paralleling the analogous ligand *N*,*N*′-bis(2-picolyl) ethylene diamine with pyridine moieties (Bispicen, $\log\beta_{CuL}$ 16.30) [35]. Notably, ligands like poly(2-imidazolylmethyl)amine and similar counterparts have been patented for forming metal complexes with radionuclides [36]. Recent BisIM, along with tris and tetra-imidazole ligands, have also been explored as inhibitors of metallo-β-lactamases based on their affinity for Zn^{2+} ions [32].

In this study, we present a potentiometric and spectroscopic analysis of copper(II)/polyimidazole ligands, TrisIM (N,N,N′-tris((imidazol-4-yl) methyl)-ethylenediamine), TetraIM (N,N,N,N′-tetra((imidazol-4-yl)-methyl)-ethylenediamine) (Fig. 1) and an investigation of BisIM, TrisIM and TetraIM anticancer activities towards CaCo-2 (colorectal adenocarcinoma), SH-SY5Y (neuroblastoma) and K562 (chronic myelogenous leukemia) cell lines. We compared the cytotoxic activity of polyimidazole ligands and their copper(II) complexes with the analogous polypyridine ligands, Bispicen, Trispicen and TPEN. The antiproliferative effect of TetraIM on K562 cells was studied further concerning the apoptotic pathway activation.f

2. Materials and methods

2.1. Materials

Bispicen and TPEN have been purchased from TCI. Trispicen, BisIM, TrisIM and TetraIM have been synthesized as previously reported [32,37].

Dulbecco's modified Eagle's medium (DMEM), RPMI 1640 medium and fetal bovine serum were from Euroclone. Acridine orange (CCCP, carbonyl cyanide *m*-chlorophenylhydrazone), dithiotreitol (DTT), ethidium bromide, MTT [3-(4,5-dimethylthiazol-2-yl)-2,5-diphenyltetrazolium bromide], Triton X-100 and tert-butyl hydroperoxide (t-BHP), were purchased from Sigma-Aldrich. 2′,7′-dichlorofuorescein diacetate ($DCFH_2$-DA) was purchased from Cayman Chemical and JC-1 was from Molecular Probes.

Fluorogenic caspase substrates, acetyl-Asp-Glu-Val-aspaminomethylcoumarin (Ac-DEVD-AMC), acetyl-Ile-Glu-Thr-Asp-aminotrifluoromethylcoumarin (Ac-IETD-AFC) and acetyl-Leu-Glu-His-Asp-aminomethylcoumarin (Ac-LEHD-AMC) were from Alexis Biochemicals. All other chemicals were reagent grade.

2.2. Potentiometry

Protonation and complex-formation constants were obtained from pH-metric titration curves registered at T = 298.2 K and ionic strength 0.1 M (KCl). The potentiometric apparatus was previously described [38]. Sample solutions containing millimolar concentrations of the reagents in different ratios were titrated with 0.1 M carbonate-free KOH. The electrode was daily calibrated for hydrogen ion concentration by titrating HCl with the standard base solution under the same experimental conditions as above and potentiometric data were processed using the SUPERQUAD [39] and Glee [40] programs. The purities and exact concentrations of the ligand solutions were determined by the Gran method [41]. The HYPERQUAD [42] program was employed for the overall formation constant (β) calculations, referred to the following equilibrium equation: pM + qL + rH ⇆ MpLqHr (charges omitted; p is 0 in the case of ligand protonation; r can be negative). The computed standard deviations (referring to random errors only) were given by the program itself and are shown in parentheses as uncertainties on the last significant digit. Hydrolysis constants for the Cu(II) ion were taken from the literature [43] (charges omitted): $\log\beta(CuH_{-1})$ = −7.7; $\log\beta(Cu_2H_{-2})$ = −10.75; $\log\beta(Cu_3H_{-4})$ = −21.36; $\log\beta(CuH_{-4})$ = −39.08. The distribution and competition diagrams were computed using the HYSS program [44].

2.3. Spectrophotometric measurements

The absorption spectra of Cu^{2+} solutions were recorded on a Varian Cary50 Probe spectrophotometer, in the range 350–850 nm, using a quartz cuvette with an optical path of 1 cm at room temperature. The composition of the sample solutions was similar to that employed in potentiometry.

2.4. Cell culture

The human CaCo-2 (colorectal adenocarcinoma), SH-SY5Y (neuroblastoma), K562 (chronic myelogenous leukemia) and HaCaT (keratinocyte) cell lines were obtained from the American Type Culture Collection. The CaCo-2, SH-SY5Y and HaCaT cells were grown in DMEM medium, while the K562 cells were cultured in RPMI 1640 medium. The media were supplemented with 10% heat-inactivated fetal bovine serum, 100 U/mL penicillin, 100 μg/ mL streptomycin and 2 mM glutamine. Cells were maintained at 37 °C in a humidified 5% CO_2 atmosphere. Cell viability was determined by trypan blue exclusion test.

2.5. Cytotoxicity assay

The effects of compounds on cell viability were evaluated *in vitro* using the MTT colorimetric method [45]. Exponentially growing cells were seeded in 96-well plates and, after 24 h of growth, were exposed to increasing concentrations of compounds for 48 h in the presence or absence of 20 μM $CuCl_2$. After treatment, the MTT reagent, at a final concentration of 0.5 mg/mL, was added to each well and the cells were incubated for an additional 3 h at 37 °C. The formazan crystals were dissolved by the addition of acidified isopropanol (0.04 N HCl in isopropanol). The absorbance at 570 nm was quantified on a microplate reader (Infinite M Plex, Tecan). Cell survival was determined by comparing the absorbance of treated and untreated cells; the viability of untreated cells was considered 100%. The IC_{50} was calculated using graphs generated from Microsoft Excel.

2.6. Apoptosis evaluation

Acridine orange/ethidium bromide double staining was used to visualize nuclear morphological changes characteristic of apoptosis. After washing with PBS, cells were stained with a fluorescent solution containing 100 μg/mL ethidium bromide and 100 μg/mL acridine orange in PBS and immediately observed under a fluorescence microscope. A minimum of 400 cells were counted to quantify apoptosis for each sample. Cells showing condensed and fragmented chromatin were considered apoptotic.

2.7. Caspase activity

After treatments, cells were washed three times with ice-cold PBS and solubilized in lysis buffer containing 50 mM Tris-HCl, pH 7.4, 10 mM EGTA, 1 mM EDTA, 1% (*v*/v) Triton X-100, for 30 min at 4 °C. The lysates were clarified by centrifugation at 4 °C at 13,000 x g for 15 min. Protein aliquots (60 μg) were incubated with 20 μM fluorogenic caspase peptide substrate, Ac-DEVD-AMC (for caspase-3) for 30 min, Ac-IETD-AFC (for caspase-8) and Ac-LEHD-AMC (for caspase-9) for 1 h, in the reaction buffer (50 mM Tris–HCl, pH 7.4, 10 mM EGTA, 1 mM EDTA, 10 mM DTT), at 37 °C [46]. Fluorescence was measured on a Perkin-Elmer LS-50B spectrofluorometer, setting excitation at 380 nm and emission at 460 nm for caspase-3 and -9 and setting excitation at 400 nm and emission at 505 nm for caspase-8.

2.8. Detection of intracellular reactive oxygen species (ROS)

DCF fluorescence was used to detect the generation of cellular ROS [47]. K562 cells were exposed to 50 and 100 μM TetraIM for 48 h at 37 °C and to 100 tert-butylhydroperoxide (t-BHP) for 1 h at 37 °C as a positive control. After treatments, 2×10^5 cells were incubated with $DCFH_2$-DA to a final concentration of 20 μM at 37 °C for 30 min. After washing with PBS, the fluorescence intensity of cells was analyzed with a Perkin–Elmer LS-50B spectrofluorometer, setting excitation at 502 nm and emission at 523 nm.

Table 1
Protonation constants at $I = 0.1$ M (KCl), $T = 25$ °C.

	BisIM[a]	TrisIM		TetraIM		
Species	log*K*	log*β*	log*K*	log*β*	log*K*	group
HL^{+}	9.05	8.97(2)	8.97	8.42(2)	8.42	amine
H_2L^{2+}	6.56	15.39(2)	6.42	14.99(3)	6.58	amine
H_3L^{3+}	4.26	20.14(2)	4.75	20.36(3)	5.37	Im
H_4L^{4+}	3.21	22.71(3)	2.57	24.03(4)	3.67	Im

[a] Protonation data for BisIM are from [34,35].

2.9. Detection of Mitochondrial Transmembrane Potential (ΔΨm)

The fluorescent dye JC-1 was used to analyze changes in mitochondrial membrane potential. After treatments, 5×10^5 cells were labeled with 2 μM JC-1 for 30 min at 37 °C; then cells were washed twice with a warm serum-free medium and resuspended in 500 μL RPMI 1640 without phenol red for spectrofluorimetric analysis [48].

The red fluorescence in excitation/emission (488 nm/595 nm) and green fluorescence in excitation/emission (488 nm/535 nm) were measured using a Perkin-Elmer LS-50B spectrofluorometer. Then, the red/ green fluorescence intensity ratio, which allows the characterization of mitochondrial function, was determined. The protonophore carbonyl cyanide *m*-chlorophenylhydrazone (50 μM CCCP) was used as a positive control for potential disruption.

2.10. Statistical analysis

Biological data are reported as mean ± SD. Statistical differences were calculated using the Student's *t*-test. Results were considered statistically significant at *p*-value <0.05.

3. Results and discussion

The complexing properties of TrisIM and TetraIM were studied by potentiometry and UV–Vis spectroscopy. Protonation and complexation constants of BisIM have been reported elsewhere [34,35].

Cu/polypyridine systems have been widely investigated elsewhere, and complex stability constants and complex copper(II) structures have been reported [21,35,49,50].

3.1. Protonation equilibria of TrisIM and TetraIM

Four protonation constants have been measured for both investigated ligands (Table 1); the third and fourth imidazoles of TrisIM and TetraIM are too acidic to be protonated in the explored pH range (2.5–10.5) and the corresponding equilibria could not be detected by potentiometry.

3.2. Complex-formation equilibria with Cu^{2+}

3.2.1. Spectrophotometry

Differently from Cu^{2+}/BisIM complex ($\lambda_{max} = 580$ nm, Martins et al. [34]), the absorption bands for Cu^{2+}/TrisIM solutions, recorded at variable pH, are located around 640–660 nm, almost unchanged from pH 4 to pH 10, with only a modest blue shift; this behaviour is the same at both 1:1 and 2:1 metal/ligand ratios (Fig. 2). This λ_{max} value, higher than that recorded in the case of $[Cu(BisIM)]^{2+}$ complex, is in keeping with the pentaamine effect reported elsewhere [51], and it is also

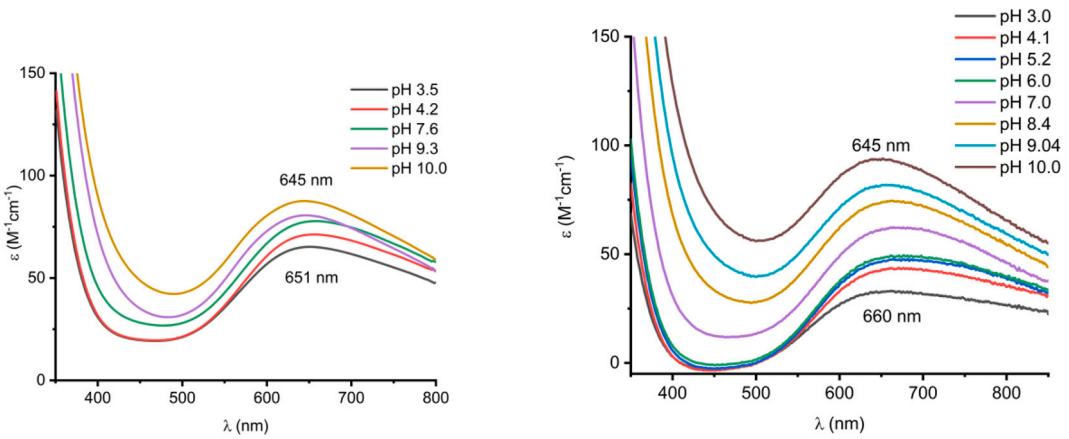

Fig. 2. Uv-Vis spectra at variable pH of Cu^{2+}/TrisIM solutions. On the left: M/L concentration ratio = 1:1, $C°_M$ = 0.65 mM; on the right: M/L concentration ratio = 2:1, $C°_M$ = 0.85 mM.

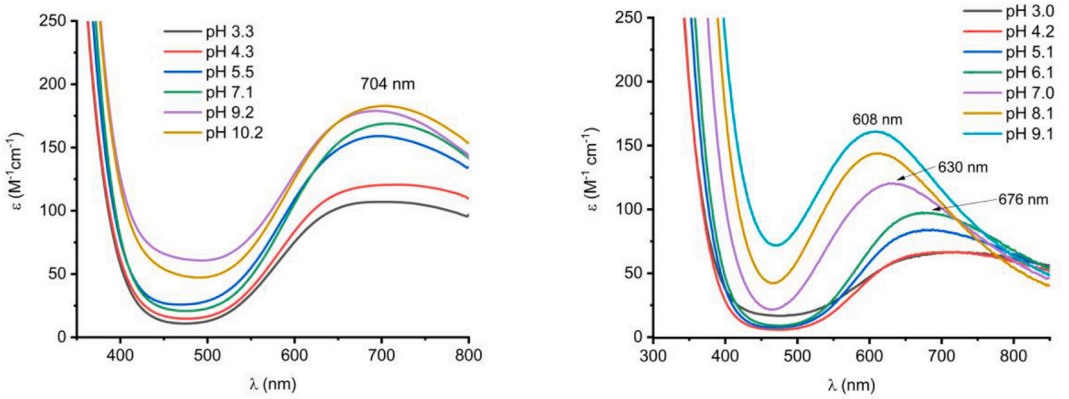

Fig. 3. Vis spectra at variable pH of Cu^{2+}/TetraIM solutions. On the left: M/L concentration ratio = 1:1, $C°_M$ = 0.66 mM; on the right: M/L concentration ratio = 2:1, $C°_M$ = 0.86 mM.

compatible with the hypothesis of a mixture of (N_{im}, N_{amine}, $2H_2O$), ($2N_{amine}$, $2H_2O$) and ($2N_{im}$, N_{amine}, H_2O) planar or elongated octahedral structures (predicted λ_{max} = 673, 663 and 617 nm, respectively) [52]. Spectrophotometric data exclude the formation of (4 N) species, with four nitrogen atoms bound to the same metal ion (predicted λ_{max} < 580 nm).

Otherwise, in the case of the Cu^{2+}/TetraIM system, we observed two different spectrophotometric behaviours. When the M/L concentration ratio is 1:1 (Fig. 3, left), the position of the absorption band is fixed around 700 nm, thus suggesting a (2 N) geometry in the equatorial plane (predicted λ_{max} = 663–687 nm, eventually "red-shifted" to higher wavelengths by the axial coordination of further imidazole nitrogens [52]). On the basis of the present experimental data, it is not possible to identify the specific groups involved in complexation, but, most likely, a mixture of species exists with different nitrogen combinations. The binding of three or four nitrogen atoms in the equatorial plane of the complex seems to be excluded throughout all the pH range.

On the other hand, when the M/L concentration ratio is 2:1 (Fig. 3, right), a not negligible blue shift is observed when the solution pH is increased (along with precipitation at pH higher than 9). This behaviour could be ascribed to the formation of binuclear species, where the second Cu^{2+} ion can bind up to three nitrogen atoms in the squared equatorial plane, possibly with coordination (N_{im}, $2N_{amine}$, H_2O) (predicted λ_{max} = 605 nm). A similar species has been reported for TPEN copper complexes [50].

Table 2
Complex-formation constants with Cu^{2+} at I = 0.1 M (KCl), T = 25 °C.

	BisIM[(a)]	BisIM[(b)]	TrisIM		TetraIM	
Species	logβ	logβ	logβ	log$K$	logβ	log$K$
$[CuH_2L]^{4+}$	–	–	–	–	23.3(5)	–
$[CuHL]^{3+}$	–	–	19.05(3)	–	21.1(4)	2.2
$[CuL]^{2+}$	16.5	16.65	15.77(2)	3.28	15.7(4)	5.4
$[CuH_{-1}L]^{+}$	–	–	5.84(3)	9.93	5.4(4)	10.3
$[Cu_2L]^{4+}$	–	–	–	–	18.4(7)	–
$[Cu_2H_{-2}L]^{2+}$	–	–	–	–	5.8(4)	–
n_p			200		250	
σ			3.5		5.3	

[(a)] [35]; [(b)] [34].

3.2.2. *Potentiometry of Cu^{2+}/TrisIM complexes*

Potentiometric studies on Cu^{2+}/TrisIM solutions suggested the formation of only variously protonated, mononuclear complexes, with 1:1 stoichiometry (see Table 2), also in the presence of an excess of ligand or metal ion. The distribution diagram of Fig. 4 shows that the main species, formed in a wide pH range around neutrality, is the complex $[CuL]^{2+}$, in good agreement with what was reported in previous studies on BisIM copper complexes [34]. Precipitation was observed in the case of a metal/ligand ratio of 2:1 (C_M = 1 mM), around pH 6.5.

The first species detected at the lowest limit of the pH range is $[CuHL]^{3+}$; this complex reaches its formation maximum around pH 3 where it bounds about the 60% of all the Cu(II) ion available in solution (Fig. 4). Its stoichiometry implies that only one nitrogen atom of the

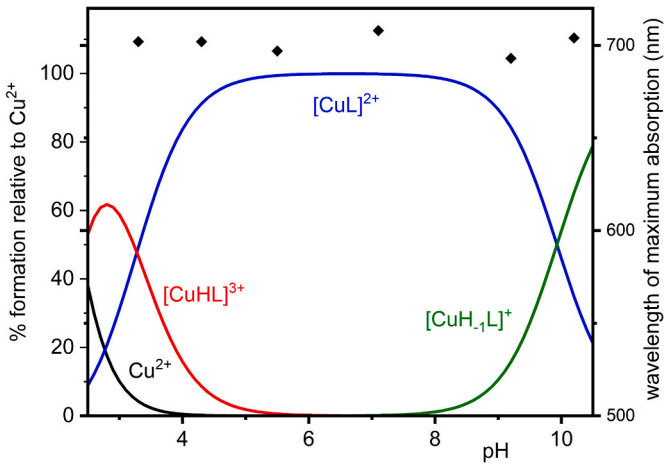

Fig. 4. Distribution diagram of Cu^{2+} complexes with TrisIM and corresponding λ_{max} values of the Vis spectra (diamond symbols scaled on the right axis). $C^{\circ}_M = C^{\circ}_L = 0.65$ mM.

ligand is protonated, most likely that of the most basic amino group of the backbone. Nonetheless, if the second amine and all the imidazole side groups are deprotonated at a pH as low as 3, two or three of them should be bound to the metal ion. This behaviour can justify the spectrophotometric results showing a wide absorption band centred around a λ_{max} value of 653 nm. When pH is increased, the last proton is released, with a log*K* value of 3.28 (Table 2). Since this proton was bound to the second amino group, the log*K* value suggests the coordination to copper in substitution of one imidazole. In fact, only a modest blue shift is observed (from 653 to 640 nm), as expected by the substitution of a "weaker" imidazole nitrogen atom by a "stronger" amine nitrogen; on the other hand, this blue shift is too low to suggest the formation of a 4 N complex, whose wavelength of maximum absorption would be much lower than 600 nm, as observed in the Cu^{2+}/BisIM system [34]. The last deprotonation step, observed in the alkaline pH range, can be ascribed to a water molecule of the inner hydration sphere of Cu^{2+}.

If the metal-to-ligand ratio is raised to 2:1, the behaviour is the same, taking into account that the excess of copper remains uncomplexed, giving rise to precipitation at pH 6.5 (**not shown**).

3.2.3. *Potentiometry of Cu^{2+}/TetraIM complexes*

In the case of the Cu^{2+}/TetraIM system, when the metal ion and ligand concentrations are equimolar, the situation is similar to that described above for TrisIM (from the point of view of the stoichiometry of the formed complexes), except for the fact that the additional diprotonated $[CuH_2L]^{4+}$ species has been detected at the most acidic pH values. This is not surprising since TetraIM contains one more imidazole group than TrisIM. The main species at neutral pH is again the $[CuL]^{2+}$ complex (Fig. 5, left).

In the presence of an excess of copper ion, binuclear species are formed, which can bind the additional metal ion and avoid the formation of insoluble species till pH 9 (Fig. 5, right). The species distribution is deeply affected by the formation of the binuclear complex $[Cu_2H_{-2}L]^{2+}$ above pH 6, which quickly becomes the most abundant species in solution, practically involving all the metal ions in the alkaline pH range. This species is certainly responsible for the unexpected changes in the Vis spectra described above.

3.3. *Comparison of the complexing ability of polyimidazole ligands*

An evaluation of the overall strength of the investigated ligands to stably coordinate the Cu^{2+} ion can be obtained through a competition diagram, calculated - in the whole explored pH range - from the determined stability constants of the binary metal complexes with each ligand. The diagram reported in Fig. 6 refers to a hypothetical solution

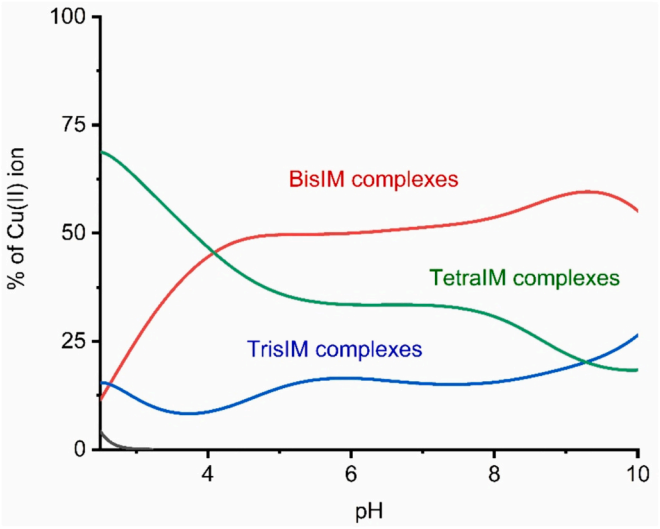

Fig. 6. Calculated competition diagram on a solution containing Cu^{2+}, BisIM, TrisIM and TetraIM, all of them 1 mM. Only the formation of binary complexes is hypothesized.

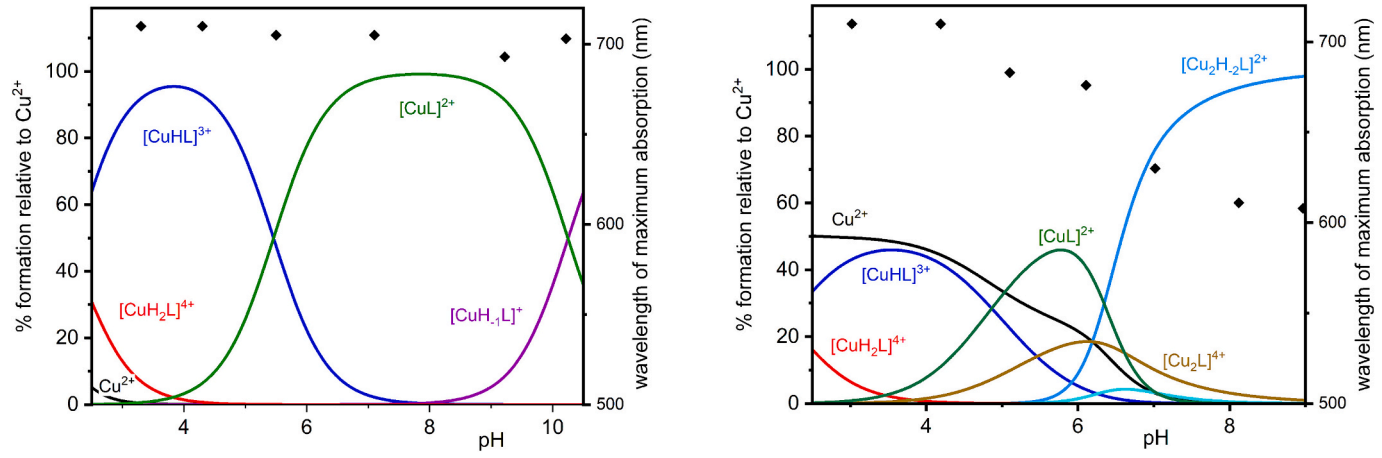

Fig. 5. Distribution diagrams of Cu^{2+} complexes with TetraIM and corresponding λ_{max} values of the Vis spectra (diamond symbols scaled on the right axis). On the left: $C^{\circ}_M = C^{\circ}_L = 0.66$ mM. On the right: $C^{\circ}_M = 0.86$ mM; M/L 2:1 ratio.

Table 3
Cytotoxic activities of polyimidazole and polypyridine ligands. The given values are the IC_{50} (concentration of compounds that inhibited cell growth by 50%) expressed in μM.

Compound	K562	CaCo-2	SH-SY5Y	HaCaT
BisIM	> 100	> 100	> 100	> 100
BisIM +20 μM $CuCl_2$	> 100	> 100	> 100	> 100
TrisIM	> 100	> 100	> 100	> 100
TrisIM +20 μM $CuCl_2$	> 100	> 100	> 100	> 100
TetraIM	53.0 ± 5.3	> 100	> 100	> 100
TetraIM +20 μM $CuCl_2$	> 100	> 100	> 100	> 100
Bispicen	10.6 ± 0.5	> 80	59.3 ± 2.1	22.1 ± 2.1
Bispicen +20 μM $CuCl_2$	34.6 ± 3.1	> 80	72.4 ± 3.2	57.0 ± 6.3
Trispicen	7.3 ± 0.7	6.9 ± 0.4	8.7 ± 1.7	6.2 ± 0.3
Trispicen +20 μM $CuCl_2$	> 16	> 16	> 16	14.8 ± 1.0
TPEN	6.5 ± 0.2	6.9 ± 0.2	7.8 ± 0.3	6.5 ± 0.4
TPEN +20 μM $CuCl_2$	> 16	> 16	> 16	> 16

Results represent the mean ± SD of three independent experiments.

containing equimolar concentrations of the metal ion, BisIM, TrisIM and TetraIM. At the most acidic pH values, TetraIM proves to be the most effective ligand, most likely due to its higher number of imidazole groups acting as anchoring sites for the copper ion. However, at pH >4, the $[CuL]^{2+}$ complex formed by BisIM dominates the system due to the ability of this ligand to bind the metal ion in a very stable (4 N) mode. TetraIM is a better ligand than TrisIM around neutral pH, and this property can be again ascribed to its higher number of imidazole groups, which allow more different combinations of binding atoms in the complex-formation equilibria.

3.4. Effects on cancer cell growth and viability

The effect of polyimidazole ligands, BisIM, TrisIM, and TetraIM, on the growth and viability of CaCo-2, SH-SY5Y and K562 cancer cells was compared to that of polypyridine ligands, Bispicen, Trispicen and TPEN. The ligands were studied alone and in the presence of $CuCl_2$. Stability constants for polyimidazole ligands reported above were used to obtain speciation in the presence of copper(II). As for polypyridine ligands, stability constants reported elsewhere were used [21,35].

The calculations at different ligand concentration values in the range 6.25–100 μM, with a Cu^{2+} concentration of 20 μM at pH 7.4, showed that, for all the polyimidazole and polypyridine ligands, the only formed complex is always the species $[CuL]^{2+}$, which involves all the metal ion in solution when the ligand is equimolar to copper or in excess; only in the case of TetraIM, the binuclear species $[Cu_2H_{-2}L]^{2+}$ is also formed at the lowest ligand concentration.

Cells were exposed to increasing concentrations (from 6.25 to 100 μM for BisIM, TrisIM and TetraIM; from 5 to 80 μM for Bispicen; from 1 to 16 μM for Trispicen and TPEN) of compounds for 48 h, in the presence or absence of 20 μM $CuCl_2$. Then, cell survival, compared with untreated controls, was evaluated using the MTT assay. The IC_{50} values obtained are summarized in Table 3.

Cell viability of all cell lines was almost unaffected by the presence of BisIM and TrisIM.

BisIM, despite IC_{50} values >100 μM, showed a mild cytotoxic activity only on SHSY-5Y cells at the concentrations of 50 and 100 μM, with a 24% and 28.3% reduction of viability, respectively. TetraIM induced a significant antiproliferative effect in K562 cells with an IC_{50} value of 53 μM, but it did not show any relevant cytotoxic activity in the other cell lines.

A stronger antiproliferative effect was instead induced by polypyridine ligands, mainly by Trispicen and TPEN, with IC_{50} values ranging from 6.2 to 8.7 μM for all tested cells. A different behaviour among the cell lines was observed in the cytotoxic effect of Bispicen; a higher susceptibility was found in K562 cells with an IC_{50} value of 10.6 μM, while CaCo-2 cells were less responsive to the Bispicen activity.

Although the effect of these ligands on normal peripheral blood

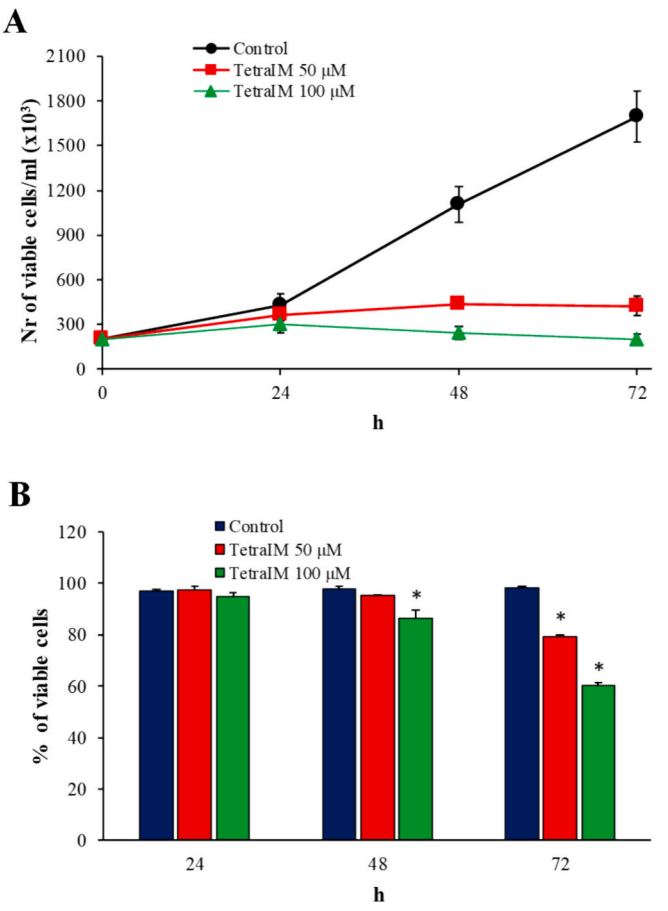

Fig. 7. Effect of 50 and 100 μM TetraIM on K562 cell growth (A) and viability (B). Untreated or TetraIM-treated cells were counted at the indicated time and the percentage of trypan blue negative K562 cells after exposure to TetraIM was determined. Results represent the mean ± SD of three independent experiments. *Data are significantly different from untreated control ($p < 0.05$). (For interpretation of the references to colour in this figure legend, the reader is referred to the web version of this article.)

lymphocytes has previously been studied [28,32], the experiments were also carried out under the same experimental conditions on a different type of normal cells, the human keratinocyte HaCaT cell line. Polyimidazole ligands showed no significant effects on HaCaT cell viability, whereas, with polypyridine ligands, cytotoxic activity was also observed in normal cells with IC_{50} values similar to those of cancer cells. This result confirms the toxic behaviour of polypyridine ligands described towards normal peripheral blood lymphocytes [28,32], while BisIM and TetraIM proved to be less active on HaCaT cells than on lymphocytes.

Since cytotoxicity induced by both TetraIM and polypyridine ligands was always reduced by the addition of 20 μM $CuCl_2$, which prevents the chelation of intracellular metals, it can be hypothesized that their activity was mainly due to the extraction of essential metals, especially copper, but also iron and zinc, from enzymes involved in several biological processes.

As for TPEN complex with copper, iron and zinc have been investigated and copper complex showed the highest stability ($\log\beta_{CuL} = 20.6$, $\log\beta_{ZnL} = 15.6$ and $\log\beta_{FeL} = 14.6$) [53]. A similar trend can be hypothesized for other ligands in keeping with the Irving Williams series [54].

Polypiridine ligands were the most active compounds in this study and their antiproliferative mechanism has been investigated [19–21,55]. We studied the selective antiproliferative mechanism of TetraIM that induced cell death only in leukemic K562 cells without affecting the viability of normal keratinocyte cells.

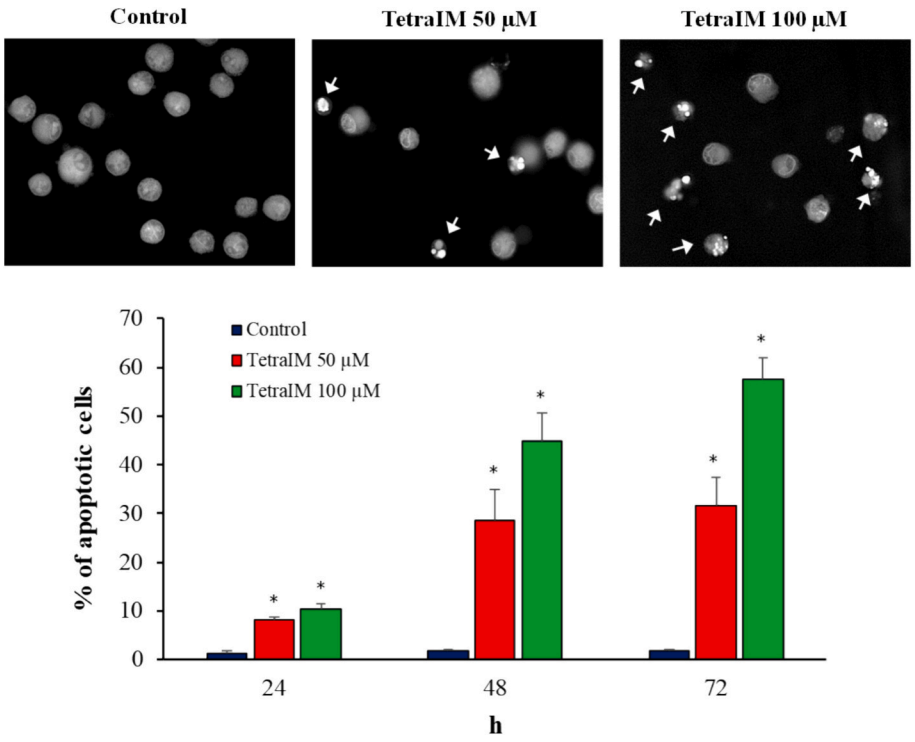

Fig. 8. Effect of TetraIM on K562 apoptosis. Analysis of nuclear morphological features of apoptosis. The percentage of condensed and fragmented nuclei was estimated by fluorescence microscope analysis of acridine orange and ethidium bromide double-stained cells observed at the indicated times. Results represent the mean ± SD of three independent experiments. *Data are significantly different from untreated control ($p < 0.05$). The *insert* shows representative microscope pictures of K562 cells after 72 h of treatments; arrows indicate apoptotic cells. (For interpretation of the references to colour in this figure legend, the reader is referred to the web version of this article.)

The effect of 50 and 100 µM TetraIM on K562 cell growth and viability was also evaluated by trypan blue exclusion test after 24, 48 and 72 h of treatment.

During the first 24 h of incubation, 50 and 100 µM TetraIM treatments induced only a mild decrease of cell growth compared to untreated cells; afterward, an almost full block of growth was observed (Fig. 7A). After 72 h of 50 and 100 µM TetraIM exposure, the amount of dead cells was around 20% and 40%, respectively (Fig. 7B).

3.5. TetraIM-induced apoptosis in K562 cells

To determine the mechanism by which TetraIM inhibited K562 cell growth and exerted its cytotoxic effects, treated K562 cells were analyzed for changes in nuclear morphology typical of apoptosis.

TetraIM-treated K562 cells exhibited a progressive increase of apoptotic cells upon 24 h of treatment, which reached about 30% and 57% of apoptotic cells after 72 h with 50 and 100 µM, respectively (Fig. 8).

The occurrence of the apoptotic process was confirmed by measuring the activity of the caspase-3 enzyme, which plays a crucial role during the apoptotic process and is a key element in the execution phase of apoptosis. In K562 cells, TetraIM treatment induced a significant increase of caspase-3 activity that reached a 22.5-fold value with a concentration of 50 µM and a 48.4-fold value with a concentration of 100 µM, as compared to control untreated cells after 72 h of incubation (Fig. 9A).

Since apoptotic cell death is regulated by either the extrinsic and the intrinsic pathways, activated by the "initiator", caspase-8 or caspase-9, respectively, to examine further the mechanism of TetraIM-induced apoptosis, its effect on the activation of initiator caspases was investigated. Significant increases, with similar time courses, of both caspase-8 and caspase-9 activities were observed (Fig. 9B, C). The near simultaneous activation of both caspase-9 and caspase-8 in K562 cells suggests that apoptosis could be induced through a cross-talk between the extrinsic and the intrinsic pathways that led to mitochondrial depolarization and activation of effector caspase-3.

3.6. ROS generation and alteration in mitochondrial membrane potential ($\Delta\Psi m$)

To investigate the mechanisms associated with TetraIM cytotoxicity, the involvement of reactive oxygen species (ROS) and changes in mitochondrial membrane potential were studied. Intracellular ROS accumulation was tested by using the ROS-sensing fluorescent probe DCFH-DA. A significant dose-dependent increase of intracellular ROS, about 3 and 7.5-fold, after 48 h of treatment with 50 and 100 µM TetraIM, respectively, was observed (Fig. 10). This result suggests that TetraIM-induced apoptosis could be due not only to metal depletion but also to the significant increase in intracellular ROS with a mechanism like that described for TPEN [25]. TetraIM-Cu complexes could be redox-active and react with O_2 to produce anion superoxide and H_2O_2, contributing to alteration in the redox homeostasis and triggering cell toxicity and death. The involvement of mitochondria in TetraIM-induced apoptosis was determined by measuring alteration in the mitochondrial membrane potential (MMP) by JC-1 dye.

JC-1 is a dual-emission dye that can exist as either a green fluorescence monomer in depolarized mitochondria of unhealthy/apoptotic cells or a red fluorescence aggregate in polarized mitochondria of healthy cells, allowing the measurement of the degree of mitochondrial polarization status through the red/green fluorescence ratio [48].

A significant dose-dependent decrease in the ratio of red-green fluorescence intensity, indicating depolarization of mitochondrial membranes, was observed after 48 h of treatment (Fig. 11).

This result confirms the involvement of the intrinsic pathway in apoptosis activation.

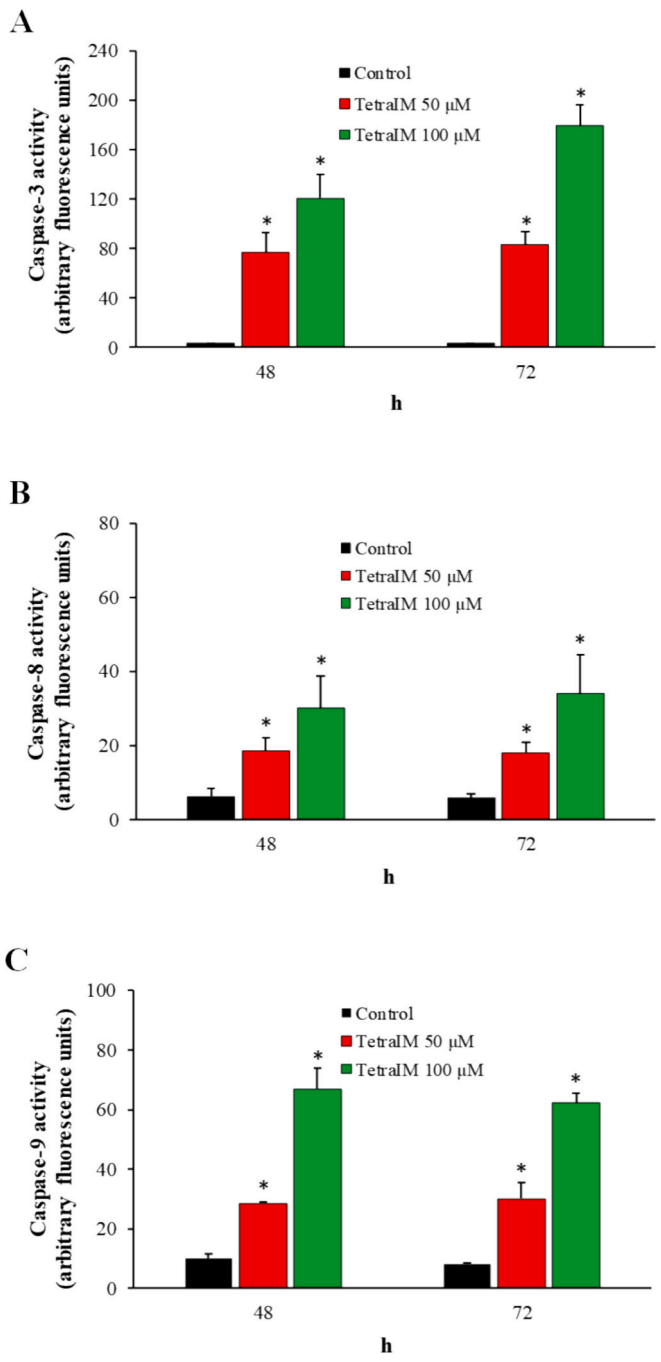

Fig. 9. Caspase-3 (A), caspase-8 (B) and caspase-9 (C) activities. The caspase activities were measured in the cytosol of K562 untreated and TetraIM-treated cells by using Ac-DEVD-AMC, Ac-LEDH-AMC and Ac-IETD-AFC as substrates, respectively. Results represent the mean ± SD of three independent experiments. *Data are significantly different from untreated control ($p < 0.05$). (For interpretation of the references to colour in this figure legend, the reader is referred to the web version of this article.)

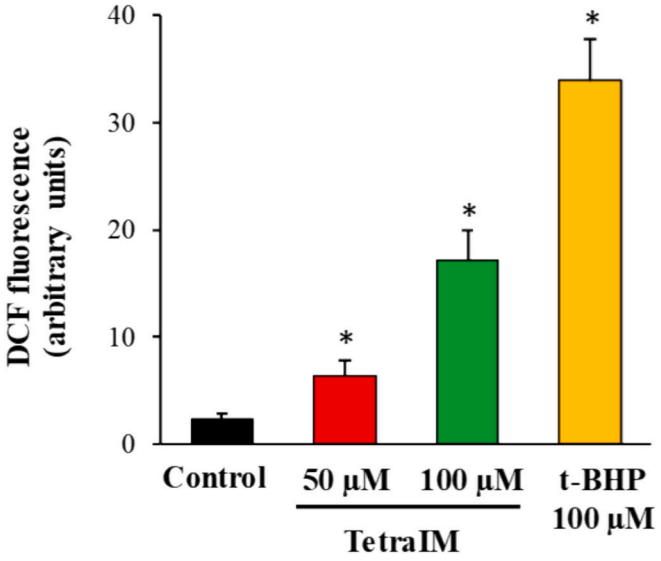

Fig. 10. ROS production in K562 cells untreated or treated for 48 h with TetraIM or for 1 h with 100 µM tert-butylhydroperoxide (t-BHP) as the positive control. After incubation with 10 µM $DCFH_2$-DA for 30 min, DCF fluorescence was determined by spectrofluorimetric analysis. Results represent the mean ± SD of three independent experiments. *Data are significantly different from untreated control ($p < 0.05$).

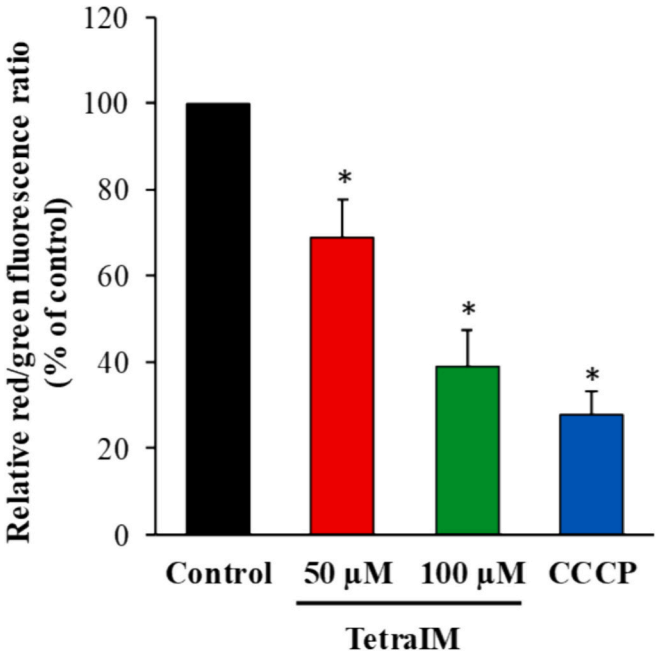

Fig. 11. Analysis of changes in mitochondrial membrane potential of K562 cells after TetraIM treatment. Red/green fluorescence ratio analysis after JC-1 staining. Incubation with 50 µM CCCP for 5 min was used as a positive control for potential disruption. Results represent the mean ± SD of three independent experiments. *Data are significantly different from untreated control ($p < 0.05$).

4. Conclusions

We studied the complexation properties of tris and tetraimidazole ligands, which can form copper complexes with high stability constants. Although their copper-complexation capability, the polyimidazole ligands are less cytotoxic than the analogous polypyridine ligands. The toxicity of polyimidazole and polypyridine ligands was reduced in the presence of copper(II). Nevertheless, polypyridine ligands carry out their activity extensively and not selectively, being equally active on cancer and normal cells. TetraIM, the only polyimidazole ligand active on a cancer cell line, induced caspase-dependent apoptosis with an increase in intracellular ROS production and mitochondrial damage in leukemic K562 cells. This mechanism may be associated with copper chelation, leading to redox dyshomeostasis, as widely reported [56,57]. The chelation of iron or zinc cannot be excluded even if the reported stability constants of polypyridine ligands are lower than those for

copper(II), in keeping with the Irving Willimas series.

The low cytotoxicity of the polyimidazole ligands, even if it limits their use as anticancer agents, makes them promising for other medical applications, such as in the treatment of metal overload, microbial infections, inflammation, or neurodegenerative disorders. Further studies will be necessary to evaluate other possible uses of these compounds.

CRediT authorship contribution statement

Fabrizia Brisdelli: Writing – review & editing, Writing – original draft, Methodology, Investigation, Formal analysis, Data curation. **Noemi Bognanni:** Writing – original draft, Investigation. **Alessandra Piccirilli:** Writing – original draft, Investigation. **Mariagrazia Perilli:** Writing – review & editing, Formal analysis, Data curation. **Denise Bellotti:** Writing – original draft, Methodology, Investigation, Formal analysis, Data curation. **Maurizio Remelli:** Writing – review & editing, Writing – original draft, Methodology, Investigation, Formal analysis, Data curation. **Graziella Vecchio:** Writing – review & editing, Writing – original draft, Supervision, Methodology, Funding acquisition.

Declaration of competing interest

The authors declare that they have no known competing financial interests or personal relationships that could have appeared to influence the work reported in this paper. Graziella Vecchio reports financial support was provided by Italian Ministry of Research. If there are other authors, they declare that they have no known competing financial interests or personal relationships that could have appeared to influence the work reported in this paper.

Data availability

Data will be made available on request.

Acknowledgments

The authors acknowledge support from funding within the Next-Generation EU-MUR PNRR Extended Partnership initiative on Emerging Infectious Diseases (Project no. PE00000007, INF-ACT) and PRIN (Project no. 2022JXSA9C, SPlat-G).

References

[1] H.S. Krishnan, V. Bernard-Gauthier, M.S. Placzek, K. Dahl, V. Narayanaswami, E. Livni, Z. Chen, J. Yang, T.L. Collier, C. Ran, J.M. Hooker, S.H. Liang, N. Vasdev, Mol. Pharm. 15 (2018) 695–702.
[2] L.E. Scott, C. Orvig, Chem. Rev. 109 (2009) 4885–4910.
[3] N. Puentes-Díaz, D. Chaparro, D. Morales-Morales, A. Flores-Gaspar, J. Alí-Torres, ACS Omega 8 (2023) 4508–4526.
[4] K. Gaur, A.M. Vázquez-Salgado, G. Duran-Camacho, I. Dominguez-Martinez, J. A. Benjamín-Rivera, L. Fernández-Vega, L. Carmona Sarabia, A. Cruz García, F. Pérez-Deliz, J.A. Méndez Román, M. Vega-Cartagena, S.A. Loza-Rosas, X. Rodriguez Acevedo, A.D. Tinoco, Inorganics 6 (2018) 126.
[5] G. MacDonald, I. Nalvarte, T. Smirnova, M. Vecchi, N. Aceto, A. Doelemeyer, A. Frei, S. Lienhard, J. Wyckoff, D. Hess, J. Seebacher, J.J. Keusch, H. Gut, D. Salaun, G. Mazzarol, D. Disalvatore, M. Bentires-Alj, P.P. Di Fiore, A. Badache, N.E. Hynes, Sci. Signal. 7 (2014) ra56–ra56.
[6] S. Blockhuys, P. Wittung-Stafshede, Biochem. Biophys. Res. Commun. 483 (2017) 301–304.
[7] Z. Qasem, M. Pavlin, I. Ritacco, M.Y. Avivi, S. Meron, M. Hirsch, Y. Shenberger, L. Gevorkyan-Airapetov, A. Magistrato, S. Ruthstein, Front. Mol. Biosci. 9 (2022) 1011294.
[8] W. Xie, Z. Guo, L. Zhao, Y. Wei, Prog. Mater. Sci. 138 (2023) 101145.
[9] Y. Li, IUBMB Life 72 (2020) 1900–1908.
[10] X. Shi, Y. Li, M. Jia, Z. Zhang, L. Huang, M. Zhang, Q. Xun, D. Jiang, Y. Liu, Drug Dev. Res. 84 (2023) 312–325.
[11] D. Denoyer, S. Masaldan, S.L. Fontaine, M.A. Cater, Metallomics 7 (2015) 1459.
[12] J.F. Machado, D. Sequeira, F. Marques, M.F.M. Piedade, M.J.V. de Brito, M. H. Garcia, A.R. Fernandes, T.S. Morais, Dalton Trans. 49 (2020) 12273–12286.
[13] Y. Wang, Y. Chen, J. Zhang, Y. Yang, J.S. Fleishman, Y. Wang, J. Wang, J. Chen, Y. Li, H. Wang, Drug Resist. Updat. 72 (2024) 101018.
[14] N. Chan, A. Willis, N. Kornhauser, M.M. Ward, S.B. Lee, E. Nackos, B.R. Seo, E. Chuang, T. Cigler, A. Moore, D. Donovan, M. Vallee Cobham, V. Fitzpatrick, S. Schneider, A. Wiener, J. Guillaume-Abraham, E. Aljom, R. Zelkowitz, J. D. Warren, M.E. Lane, C. Fischbach, V. Mittal, L. Vahdat, Clin. Cancer Res. 23 (2017) 666–676.
[15] H. Qi, H. Shi, M. Yan, L. Zhao, Y. Yin, X. Tan, H. Qi, H. Li, K. Weng, Y. Tang, Y. Dai, Cell Death Dis. 9 (2023) 259.
[16] D. Ramchandani, M. Berisa, D.A. Tavarez, Z. Li, M. Miele, Y. Bai, S.B. Lee, Y. Ban, N. Dephoure, R.C. Hendrickson, S.M. Cloonan, D. Gao, J.R. Cross, L.T. Vahdat, V. Mittal, Nat. Commun. 12 (2021) 7311.
[17] S.-J. Chen, C.-C. Kuo, H.-Y. Pan, T.-C. Tsou, S.-C. Yeh, J.-Y. Chang, Biochem. Pharmacol. 95 (2015) 28–37.
[18] M. Mendivil-Perez, C. Velez-Pardo, M. Jimenez-Del-Rio, Oxidative Med. Cell. Longev. 2012 (2012) 14.
[19] M. Adler, H. Shafer, T. Hamilton, J.P. Petrali, NeuroToxicology 20 (1999) 571–582.
[20] L. Rojas-Valencia, C. Velez-Pardo, M. Jimenez-Del-Rio, BioMetals 30 (2017) 405–421.
[21] S. Schaefer-Ramadan, M. Barlog, J. Roach, M. Al-Hashimi, H.S. Bazzi, K. Machaca, Bioorg. Chem. 87 (2019) 366–372.
[22] M. Mendivil-Perez, C. Velez-Pardo, L.M. Quiroz-Duque, A. Restrepo-Rincon, N. A. Valencia-Zuluaga, M. Jimenez-Del-Rio, BioMetals 35 (2022) 741–758.
[23] V.M. Kolenko, R.G. Uzzo, N. Dulin, E. Hauzman, R. Bukowski, J.H. Finke, Apoptosis 6 (2001) 419–429.
[24] F. Chai, A.Q. Truong-Tran, A. Evdokiou, G.P. Young, P.D. Zalewski, J. Infect. Dis. 182 (2000) S85–S92.
[25] M. Fatfat, R.A. Merhi, O. Rahal, D.A. Stoyanovsky, A. Zaki, H. Haidar, V.E. Kagan, H. Gali-Muhtasib, K. Machaca, BMC Cancer 14 (2014) 527.
[26] W.-Q. Ding, H.-J. Yu, S.E. Lind, Cancer Lett. 271 (2008) 251–259.
[27] M. Hashemi, S. Ghavami, M. Eshraghi, E.P. Booy, M. Los, Eur. J. Pharmacol. 557 (2007) 9–19.
[28] L. Basile, A. Piccirilli, F. Brisdelli, M. Perilli, N. Bognanni, L. La Piana, L. Principe, S. Di Bella, G. Vecchio, Results Chem. 5 (2023) 100986.
[29] W. Chen, Y. Wang, H. Wang, D. An, D. Sun, P. Li, T. Zhang, W. Lu, Y. Liu, Mol. Neurobiol. 60 (2023) 4232–4245.
[30] S. Fukuyama, Y. Matsunaga, W. Zhanghui, N. Noda, Y. Asai, A. Moriwaki, T. Matsumoto, T. Nakano, K. Matsumoto, Y. Nakanishi, H. Inoue, Allergol. Int. 60 (2011) 259–266.
[31] B. Zhu, C. Yang, L. Sun, Z. Li, J. Li, Z.-C. Hua, Metallomics 15 (2023) mfad022.
[32] N. Bognanni, F. Brisdelli, A. Piccirilli, L. Basile, L. La Piana, S. Di Bella, L. Principe, G. Vecchio, M. Perilli, J. Inorg. Biochem. 242 (2023) 112163.
[33] G. Patel, D.K. Dewangan, N. Bhakat, S. Banerjee, Curr. Res. Green Sustain. Chem. 4 (2021) 100175.
[34] J.G. Martins, R.M. Pinto, P. Gameiro, M. Teresa Barros, H.M.V.M. Soares, J. Solut. Chem. 39 (2010) 1153–1167.
[35] R.M. Smith, A.E. Martell, Critical Stability Constants, Springer, US, Boston, MA, 1975.
[36] J.W. Babich, K. Maresca, J. Kronauge, Technetium-and rhenium-Bis (Heteroaryl) complexes, And Methods Of Use Thereof (2008). US20080025915A1.
[37] L. La Piana, V. Viaggi, L. Principe, S. Di Bella, F. Luzzaro, M. Viale, N. Bertola, G. Vecchio, J. Inorg. Biochem. 215 (2021) 111315.
[38] D. Bellotti, C. Tocchio, R. Guerrini, M. Rowińska-Żyrek, M. Remelli, Metallomics 11 (2019) 1988–1998.
[39] P. Gans, A. Sabatini, A. Vacca, J. Chem. Soc. Dalton Trans. (1985) 1195–1200.
[40] P. Gans, B. O'Sullivan, Talanta 51 (2000) 33–37.
[41] G. Gran, H. Dahlenborg, S. Laurell, M. Rottenberg, Acta Chem. Scand. (1950) 559–577.
[42] P. Gans, A. Sabatini, A. Vacca, Talanta 43 (1996) 1739–1753.
[43] G. Arena, R. Cali, E. Rizzarelli, S. Sammartano, Thermochim. Acta 16 (1976) 315–321.
[44] L. Alderighi, P. Gans, A. Ienco, D. Peters, A. Sabatini, A. Vacca, Coord. Chem. Rev. 184 (1999) 311–318.
[45] T. Mosmann, J. Immunol. Methods 65 (1983) 55–63.
[46] C. Köhler, S. Orrenius, B. Zhivotovsky, J. Immunol. Methods 265 (2002) 97–110.
[47] C.P. LeBel, H. Ischiropoulos, S.C. Bondy, Chem. Res. Toxicol. 5 (1992) 227–231.
[48] F. Sivandzade, A. Bhalerao, L. Cucullo, BIO-Protoc 9 (2019) e3128.
[49] A. Lakatos, E. Zsigó, D. Hollender, N.V. Nagy, L. Fülöp, D. Simon, Z. Bozsó, T. Kiss, 39 (2010) 1302-1315.
[50] N. Hirayama, S. Iimuro, K. Kubono, H. Kokusen, T. Honjo, Talanta 43 (1996) 621–626.
[51] E.J. Billo, Inorg. Nucl. Chem. Lett. 10 (1974) 613–617.
[52] H. Sigel, R.B. Martin, Chem. Rev. 82 (1982) 385–426.
[53] G. Anderegg, E. Hubmann, N.G. Podder, F. Wenk, Helv. Chim. Acta 60 (1977) 123–140.
[54] H. Irving, R.J.P. Williams, J. Chem. Soc. Resumed (1953) 3192–3210.
[55] B. Zhu, J. Wang, F. Zhou, Y. Liu, Y. Lai, J. Wang, X. Chen, D. Chen, L. Luo, Z.-C. Hua, Cell. Physiol. Biochem. Int. J. Exp. Cell. Physiol. Biochem. Pharmacol. 42 (2017) 1822–1836.
[56] K.M. Abdullah, J.B. Kaushal, S. Takkar, G. Sharma, Z.W. Alsafwani, R. Pothuraju, S. K. Batra, J.A. Siddiqui, Heliyon 10 (2024) e27496.
[57] A. Rakshit, K. Khatua, V. Shanbhag, P. Comba, A. Datta, Chem. Sci. 9 (2018) 7916–7930.